Ecological Indicators 110 (2020) 105901

Contents lists available at ScienceDirect

Ecological Indicators

journal homepage: www.elsevier.com/locate/ecolind

Contemporary forest carbon dynamics in the northern U.S. associated with land cover changes

Wu Ma[a,b,*], Grant M. Domke[c], Christopher W. Woodall[d], Anthony W. D'Amato[a]

[a] Rubenstein School of Environment and Natural Resources, University of Vermont, Burlington, VT, United States
[b] Forest Advanced Computing and Artificial Intelligence Laboratory (FACAI), Department of Forestry and Natural Resources, Purdue University, West Lafayette, IN, United States
[c] U.S. Department of Agriculture, Forest Service, Northern Research Station, St. Paul, MN, United States
[d] U.S. Department of Agriculture, Forest Service, Northern Research Station, Durham, NH, United States

ARTICLE INFO

Keywords:
Forest
Landsat
Spatial distribution
Uncertainty
Carbon

ABSTRACT

Estimates of the spatial–temporal distributions of forest carbon (C) stocks subject to land use and cover changes is critical to greenhouse gas (GHG) estimation and reporting. Based on national forest inventory (NFI) and Landsat time series data, we applied matrix models to estimate and map spatial–temporal distributions of forest aboveground biomass (AGB) C, standing dead C, downed dead C, litter C, and soil organic C from 1990 to 2018 attributed to land cover changes and harvests in the northern United States (US). From predicted pixel-level maps, we found that all five forest C pools of northeast states and northern tier of Great Lake states had higher C density than other regions in the study area. We estimated that forest-related land cover changes reduced the forest C sink by 0.15 ton C ha^{-1} yr^{-1} (with a range of 0.12 to 0.18 ton C ha^{-1} yr^{-1}) a accounting for 29% of forest C reductions over the study period. Forests remaining forests sequestered 2.38 Pg C (2.05 to 2.61 Pg C), hence the net forest sink of the northern US increased 1.73 Pg C (1.52 to 1.93 Pg C) during 1990–2018, which is an annual rate of 0.88 ton C ha^{-1} yr^{-1} (0.77 to 0.98 ton C ha^{-1} yr^{-1}). Moreover, forest C was captured in harvested wood products by 0.33 ton C ha^{-1} yr^{-1}. An uncertainty analysis with fuzzy sets suggested that the absolute uncertainties of land cover change and harvest impacts on standing dead C, downed dead C, and litter C were lower than 4.50 ton ha^{-1} during 1990–2018. In comparison, there were high uncertainties associated with estimates of soil organic C and AGB C densities at approximately 12–40 ton ha^{-1} in northern Michigan, Wisconsin, Minnesota, and Maine, New Hampshire, and New York. This study demonstrates methods for adhering to Intergovernmental Panel on Climate Change good practice guidelines for national GHG reporting and presents spatially explicit attribution of regional trends in C fluxes to particular activities and events. The resolved estimates from this analysis can be used to examine local and regional land use and cover change policies and practices in the context of C management in the northern US.

1. Introduction

Forest ecosystems, which have the largest terrestrial carbon (C) stocks on earth, play a vital role in the global C cycle (Pan et al., 2011). Under the United Nations Framework Convention on Climate Change (UNFCCC), forest C estimates are a critical component of national-scale greenhouse gas (GHG) reporting (Woodall et al., 2015a,2015b). Forest land changes, along with natural disturbances and management activities, could play a pivotal role in altering terrestrial C fluxes and reducing atmospheric CO_2 concentrations (Zheng et al., 2011; Sleeter et al., 2018). As the most uncertain term in the C budget estimation at both global and regional scales, land-use and cover changes have been viewed as one of the largest contributors to uncertainty associated with global C emission estimates at approximately 1.0 ± 0.5 Pg C yr^{-1} since 2006 (Houghton et al., 2012; Le Quéré et al., 2016; Yu et al., 2018). The northern forest ecosystems are undergoing considerable land-use and cover changes accompanied with active forest management, which is an important driver of regional GHG balances (Ma et al., 2019). Although we have refined our understanding of the processes that influence forest C dynamics in the northern United States (US), uncertainties from the effects of land-use and cover changes and forest management activities remain large (Ollinger et al., 2002; Houghton, 2003; Canham et al., 2013; Harris et al., 2016; Sleeter et al., 2018; Alexander et al., 2018). Such large uncertainties could be reduced in

* Corresponding author at: Purdue University, 175 W State St, West Lafayette, IN 47906, United States.
E-mail address: wuma@mix.wvu.edu (W. Ma).

https://doi.org/10.1016/j.ecolind.2019.105901
Received 4 April 2019; Received in revised form 29 October 2019; Accepted 4 November 2019
1470-160X/ © 2019 Elsevier Ltd. All rights reserved.

order to strengthen the confidence in estimates included in C budget assessments and managements at regional, national, and global scales (Law et al., 2018). Therefore, an uncertainty analysis of forest C estimates is essential for contemporary assessments and management of forest C in the northern US.

Comprehensively and accurately quantifying the magnitude and spatiotemporal patterns of forest C storage and sequestration capacity is an important component of managing forest ecosystems (Cao et al., 2019). Although prior studies have improved our understanding of C exchange between forestland and non-forestland, C processes in forestland are generally underrepresented in these assessments (Hasenauer et al., 1999; Zheng et al., 2008; Zheng et al., 2011; Hasenauer et al., 2012; Neumann et al., 2015; Neumann et al., 2016a, 2016b; Ma et al., 2019). Such an outcome may be expected as simulations associated with prior studies were either limited by data availability and/or model performance. For example, numerous models lacked representation for varying forest species compositions (Zheng et al., 2013; Harris et al., 2016), while some models neglected details in harvest activities in regional modeling (Zhang et al., 2012; Williams et al., 2016). More importantly, accurate assessment of land-cover change induced forest C gain/loss often requires incorporation of high-resolution land-cover data (initial surrogate for land-use change, Woodall et al., 2015a) as forestland abandonment and expansion were substantially underestimated in past coarse-resolution land cover change maps leading to a biased and under-estimated amplitudes of forest C gain/loss (DeFries et al., 2002; Goetz and Dubayah, 2011; Zheng et al., 2011). Therefore, methods to fully integrate high-resolution land-cover data and detailed harvesting information to predict spatial–temporal C dynamics at different scales in forest ecosystems are urgently needed.

Coupled with remotely sensed data and strategic-level forest inventories, researchers have developed sophisticated models to estimate spatial–temporal distributions of forest C stocks (Dymond et al., 2002; Yan and Zhao, 2007; Kurz et al., 2009; Liang and Zhou, 2014). For example, a ForCSv2 (Forest Carbon Succession v2.0) extension for the LANDIS-II model has been applied to simulate spatially-explicit forest C succession (Dymond et al., 2002). An individual-based forest ecosystem carbon budget model (FORCCHN) has been used to investigate forest C distributions in China (Yan and Zhao, 2007). The CBM-CFS3 (Carbon Budget Model of the Canadian Forest Sector) has been developed to model C stock changes resulting from Land Use, Land Use Change, and Forestry (Kurz et al., 2009). However, traditional simulation tools in general may be restrictive due to insufficient in situ calibration and validation data and rarely considering three main components (i.e., diameter growth, mortality, and recruitment) of forest dynamics.

Matrix models, featuring a transition matrix calibrated to estimate diameter growth, recruitment, and mortality, have been applied to investigate and map forest C dynamics incorporating Landsat data and large scale in situ forest inventory data (Liang and Zhou, 2014; Ma et al., 2016, 2018a, 2018b, 2019; Ma and Zhou, 2017). For instance, a recent study by Ma et al. (2018a) developed C flux matrix models to compare size- vs. age-structured models in their capacity to predict forest C dynamics. Subsequently, Ma et al. (2018b) developed matrix models for incorporating light detection and ranging (LiDAR) strip samples and Landsat time-series, with field inventory measurements to predict forest aboveground biomass (AGB) dynamics. This study found that the use of Landsat data alone incorporating elevation, plot slope, and aspect could produce useful estimates of AGB dynamics using matrix models. To advance toward more spatially explicit estimates of forest C dynamics, Ma et al. (2019) quantified how land use changes, disturbances, and their interactions influenced future forest AGB dynamics (2018–2098) using national forest inventory (NFI) and Landsat time series data in the northern US. This research suggested that if recent trends persist, the combined effects of land use change and disturbances may serve as an important driver of C uptake and emissions in the northern US well into the 21st century. To continue this line of research, this study seeks to improve upon prior matrix models to estimate forest C dynamics (1990–2018) through explicit incorporation of harvesting and land cover change metrics building upon the breadth of Landsat and NFIs publicly available in our study area. Comparisons of the prior simulation models with empirically obtained matrix models can help reveal the best approaches for estimating spatial–temporal forest C dynamics.

The US reports estimates of economy-wide GHG emissions and removals each year from 1990 to near present as signatories to the UNFCCC (US EPA, 2018). Estimating C stocks and stock changes within the forest land category is an important part of the land sector within National GHG Inventories related to forests. As a step toward improving the spatial and temporal resolution of carbon stocks and stock change estimates for the forest land category and decreasing inventory cost in the future, the objective of this study was to characterize the impacts of land cover change and forest management (e.g., harvesting) on contemporary C dynamics (1990–2018) in the northern US. We used matrix models to better represent spatial–temporal distributions of forest C stocks considering land cover change and harvesting in addition to the refined stand dynamics modeling based on NFI and Landsat data. Specifically we (1) applied matrix models to estimate dynamics of five forest C pools including AGB, standing dead, downed dead, litter, and soil organic from 1990 to 2018; (2) quantified effects of land cover change and harvest activities on contemporary forest C dynamics (1990–2018); and (3) used fuzzy sets to represent variability in forest C dynamics resulting from uncertainties in the land cover changes and harvests across the northern US.

2. Materials and methods

2.1. Field data

Field data for this study were obtained from the NFI conducted by the US Department of Agriculture Forest Service, Forest Inventory and Analysis (FIA) program. The FIA program maintains a public-facing database (https://apps.fs.usda.gov/fia/datamart/datamart.html) of NFI data that was used in this analysis. The study covers eleven states of the northern US (Minnesota, Wisconsin, Illinois, Indiana, Michigan, Ohio, Pennsylvania, New York, Vermont, New Hampshire, and Maine) with total area of approximately 120,000,000 ha with an inventory consisting of 78,458 plots (time 1 measurement between 2008 and 2012 and remeasured 5-years later from 2013 to 2018). The area of forest land use in this study area is approximately 68,000,000 ha. For model calibration purposes, 62,766 permanent ground plots (80%) were used to estimate parameters of the matrix models and 15,692 plots (20%) were randomly selected for model validation. Each permanent ground plot is composed of four smaller fixed-radius (7.32 m) subplots spaced 36.6 m apart in a triangular arrangement around a central subplot. For each permanent ground plot, plot-level estimates of forest C pools include live tree, standing dead tree, downed dead wood, forest floor, and soil (Table 1). In addition, plot-level variables including trees per hectare, basal area per hectare, and measurements of slope, aspect, and elevation were used (Table 1).

2.2. Landsat data

Landsat time-series data were obtained from the Google Earth Engine (https://earthexplorer.usgs.gov/) and were acquired by Landsat 8 Operational Land Imager (OLI)/Thermal Infrared Sensor (TIRS), Landsat 7 Enhanced Thematic Mapper Plus (ETM +), Landsat 5 Thematic Mapper (TM), and Landsat 5 Multispectral Scanner (MSS) instruments from 2008 to 2018. Landsat 7 ETM + and Landsat 8 OLI/TIRS data were processed upon download but use predicted ephemeris, initial bumper mode parameters, or initial TIRS line-of-sight model parameters. The data were reprocessed with definitive ephemeris, updated bumper mode parameters and refined TIRS parameters, and the products were transitioned to either Tier 1 or Tier 2 and removed from

Table 1
Definitions and units of variables used in the study.

Variable	Unit	Definition/explanation
		Forest inventory data
AGB	ton ha^{-1}	Aboveground live biomass, biomass of the aboveground portion of a tree. Includes stem wood, stump, bark, top, branches, and foliage (Jenkins et al., 2003; Woodall et al., 2011).
SDC	ton ha^{-1}	Standing dead carbon, carbon in standing dead trees, including coarseroots, is estimated from models based on geographic area, forest type, and growing-stock volume (Smith and Heath, 2008; Woodall et al., 2011; Domke et al., 2011).
DDC	ton ha^{-1}	Downed dead carbon, carbon of woody material > 3 in. in diameter on the ground, and stumps and their roots > 3 in. in diameter. Estimated from models based on geographic area, forest type, and live tree carbon density (Smith and Heath, 2008).
LC	ton ha^{-1}	Litter carbon, carbon of organic material on the floor of the forest, including fine woody debris, humus, and fine roots in the organic forest floor layer above mineral soil. Estimated from models based on geographic area, forest type, and stand age (Smith and Heath, 2002).
SOC	ton ha^{-1}	Soil organic carbon, carbon in fine organic material below the soil surface to a depth of 1 m. Does not include roots. Estimated from models based on geographic area and forest type (Smith and Heath, 2008)
N	trees ha^{-1}	Number of trees per hectare
A	°	Plot aspect showing the direction to which the plot slope faces; 0 means no slope, 180 and 360 represented south- and north-facing slopes, respectively
S	°	Plot slope
E	km	Elevation
		Landsat data
TCB	W m^{-2}	Tasseled cap brightness
DI	W m^{-2}	Disturbance index
EVI	Unitless	Enhanced vegetation index
SWIR	nm	Shortwave infrared surface reflectance
TCG	W m^{-2}	Tasseled cap greenness
SAVI	Unitless	Soil adjusted vegetation index
TCA	W m^{-2}	Tasseled cap angle

the Real-Time tier (https://landsat.usgs.gov/landsat-collections).

2.3. Digital elevation model (DEM) data

Digital Elevation Model (DEM) data were obtained from the U.S. Geological Survey's (USGS) National Geospatial Program (https://www.usgs.gov/core-science-systems/national-geospatial-program/national-map) to provide physiographic variables including plot aspect, plot slope, and elevation.

2.4. Land cover change data

National Land Cover Database (NLCD) was used to quantify land cover changes during the period (2001–2011) among three primary cover types (grassland, cropland, and forestland) at a spatial resolution of 30 m across the northern US. The land cover classification system is used by NLCD2011, which is modified from the Anderson Land Cover Classification System. Forest-related land cover changes were generalized into three categories: (1) afforestation (from grassland and cropland to forestland), (2) deforestation (from forestland to grassland and cropland), and (3) forestland remaining forestland, as the C dynamics are different for each of these land cover changes.

2.5. Forest harvest data

Forest harvest data were obtained from the FIA database, which include five harvest types such as clearcut, partial, seed-tree/shelterwood, commercial thinning, timber stand improvement, and salvage cutting.

2.6. Description of the matrix models

A conventional matrix model was applied to control for diameter growth, mortality, and recruitment as follows (e.g. Buongiorno and Michie, 1980; Picard et al., 2003):

$$\mathbf{y}_{t+1} = \boldsymbol{G}_t \cdot \mathbf{y}_t + \boldsymbol{R}_t + \varepsilon \tag{1}$$

in which $\boldsymbol{y}_t$ and $\boldsymbol{y}_{t+1}$ is number of live trees per hectare at time t and $t + 1$. $\boldsymbol{G}_t$ is a transition matrix describing how trees grow or die between t and $t + 1$, respectively. $\boldsymbol{R}$ is a recruitment vector representing trees naturally recruited in the smallest diameter class between t and $t + 1$. ε is a random error.

In this study, improved matrix models were made from the traditional matrix models (Eq. (1)) by adding a vector of harvests, H_t, leading to:

$$\mathbf{y}_{t+1} = \boldsymbol{G}_t \cdot \mathbf{y}_t + \boldsymbol{R}_t + \mathrm{H}_t + \varepsilon \tag{2}$$

$\mathbf{G}_t$ and $\mathbf{G}_{it}$ are state- and time-dependent transition matrices, $\mathbf{G}_{it}$ is a submatrix of $\mathbf{G}_t$, where:

$$G_t = \begin{bmatrix} G_{1t} & & & \\ & G_{2t} & & \\ & & \ddots & \\ & & & \boldsymbol{G}_{i,t} \end{bmatrix}$$

$$\boldsymbol{G}_{it} = \begin{bmatrix} a_{i1,t} & & & & \\ b_{i1,t} & a_{i2,t} & & & \\ & \ddots & \ddots & & \\ & & b_{i,j-2,t} & a_{i,j-1,t} & \\ & & & b_{i,j-1,t} & a_{i,j,t} \end{bmatrix} \tag{3}$$

in which a_{ijt} represents the probability that a tree of species group i and diameter class j stays alive in the same size class between t and $t + 1$. The transition probability of upgrowth, b_{ijt}, represents a tree of species i and diameter class j stays alive and grows into diameter class $j + 1$ between t and $t + 1$, assuming that trees were evenly distributed within a diameter class. b_{ijt} was estimated as the annual tree diameter growth, g_{ijt}, divided by the width of the diameter class. a_{ijt} and b_{ijt} are related by:

$$a_{ijt} = 1 - b_{ijt} - m_{ijt} - h_{ijt} \tag{4}$$

where m_{ijt} is the tree mortality of species i and size class j between t and $t + 1$, h_{ijt} is the harvesting probability of species i and size class j between t and $t + 1$.

$\mathbf{R}_t$ represents number of trees naturally recruit in the smallest size class of each species group, between t and $t + 1$. $\mathbf{R}_{it}$ is a sub vector of $\mathbf{R}_t$ representing recruitment of species group i at time t, where:

$$\boldsymbol{R}_t = \begin{bmatrix} \boldsymbol{R}_{1t} \\ \boldsymbol{R}_{2t} \\ \vdots \\ \boldsymbol{R}_{m,t} \end{bmatrix} \quad \boldsymbol{R}_{it} = \begin{bmatrix} R_{it} \\ 0 \\ \vdots \\ 0 \end{bmatrix} \tag{5}$$

The annual diameter growth of the tree of species group i and size class j from t and $t + 1$ is represented by the following model (Ma et al.,

Table 2
Estimated parameters of diameter growth model, mortality model, harvest model, recruitment model, aboveground live biomass (AGB) model, standing dead carbon (SDC) model, downed dead carbon (DDC) model, litter carbon model (LC), and soil organic carbon (SOC) model.

Diameter Growth
Deciduous
$0.623^{**} - 0.182TCB^{**} - 0.592DI^{*} + 0.478EVI^{**} + 0.261SWIR^{*} - 0.849TCG^{*} + 0.971SAVI^{*} + 0.347TCA - 0.821E^{*} - 0.698S^{*} - 0.593cosA^{*} + 0.854sinA$
Coniferous
$0.696^{**} - 0.159TCB^{*} - 0.762DI^{**} + 0.321EVI^{**} + 0.864SWIR - 0.295TCG^{*} + 0.756SAVI^{**} + 0.630TCA^{*} - 0.782E^{**} - 0.347S^{**} - 0.546cosA + 0.912sinA^{*}$
Mortality
Deciduous
$0.814^{**} + 0.637TCB^{*} - 0.897DI^{**} - 0.821EVI^{**} + 0.126SWIR^{*} + 0.047TCG^{*} + 0.726SAVI^{*} - 0.357TCA - 0.851E^{*} - 0.674S^{**} - 0.813cosA + 0.871sinA$
Coniferous
$0.931^{**} + 0.513TCB^{**} - 0.864DI^{*} - 0.841EVI^{**} + 0.526SWIR^{*} + 0.846TCG + 0.334SAVI^{*} - 0.842TCA^{*} - 0.852E^{*} - 0.625S - 0.889cosA^{**} + 0.821sinA^{*}$
Harvest
Deciduous
$0.628^{*} + 0.841TCB^{*} + 0.627DI^{**} - 0.338EVI^{**} + 0.825SWIR^{*} - 0.149TCG^{*} + 0.627SAVI^{*} - 0.294TCA - 0.354E^{*} - 0.839S^{**} - 0.658cosA - 0.523sinA$
Coniferous
$0.852^{*} + 0.624TCB^{**} + 0.232DI^{**} - 0.158EVI^{*} + 0.226SWIR^{*} - 0.851TCG + 0.526SAVI^{*} - 0.269TCA^{*} - 0.620E^{*} - 0.663S - 0.552cosA^{**} - 0.116sinA^{*}$
Recruitment
Deciduous
$0.636^{***} - 0.856TCB^{*} - 0.822DI^{**} + 0.845EVI^{***} + 0.877SWIR^{**} + 0.937TCG^{*} - 0.154SAVI^{*} + 0.863TCA^{**} - 0.125E - 0.789S^{*} - 0.882cosA^{**} + 0.864sinA$
Coniferous
$0.798^{**} - 0.152TCB^{**} - 0.324DI^{*} + 0.421EVI^{**} + 0.864SWIR^{*} + 0.523TCG^{*} - 0.577SAVI^{**} + 0.811TCA - 0.327E^{**} - 0.716S^{*} - 0.742cosA^{*} + 0.547sinA$
AGB
$0.348^{***} - 0.633TCB^{**} - 0.784DI^{*} + 0.201EVI^{**} + 0.347SWIR^{*} + 0.812TCG^{**} + 0.988SAVI^{*} + 0.121TCA^{*} - 0.367E^{*} - 0.864S^{**} - 0.413cosA + 0.345sinA^{*}$
SDC
$0.135^{***} - 0.426TCB^{**} - 0.609DI^{*} + 0.152EVI^{**} + 0.234SWIR^{*} + 0.215TCG^{**} + 0.526SAVI^{*} + 0.062TCA^{*} - 0.126E^{*} - 0.217S^{**} - 0.523cosA + 0.241sinA^{*}$
DDC
$0.107^{***} - 0.125TCB^{**} - 0.523DI^{*} + 0.116EVI^{**} + 0.261SWIR^{*} + 0.269TCG^{**} + 0.856SAVI^{*} + 0.107TCA^{*} - 0.226E^{*} - 0.521S^{**} - 0.743cosA + 0.294sinA^{*}$
LC
$0.268^{***} - 0.492TCB^{**} - 0.264DI^{*} + 0.489EVI^{**} + 0.162SWIR^{*} + 0.218TCG^{**} + 0.304SAVI^{*} + 0.037TCA^{*} - 0.262E^{*} - 0.904S^{**} - 0.327cosA + 0.859sinA^{*}$
SOC
$0.083^{***} - 0.267TCB^{**} - 0.349DI^{*} + 0.115EVI^{**} + 0.341SWIR^{*} + 0.264TCG^{**} + 0.192SAVI^{*} + 0.008TCA^{*} - 0.169E^{*} - 0.327S^{**} - 0.258cosA + 0.117sinA^{*}$

Note: Significance levels: * < 0.05; ** < 0.01; *** < 0.001.

2018b; All notations defined in Table 1):

$$g_{ijt} = \alpha_{i1} + \alpha_{i2}TCB + \alpha_{i3}DI + \alpha_{i4}EVI + \alpha_{i5}SWIR + \alpha_{i6}TCG + \alpha_{i7}SAVI + \alpha_{i8}TCA + \alpha_{i9}E + \alpha_{i10}S + \alpha_{i11}cosA + \alpha_{i12}sinA + \theta_{ij} \quad (6)$$

in which α_i's are parameters to be estimated with the generalized least squares (GLS, see Rao, 1973) for diameter growth of species group i and size class j. $\theta$is an error term.

Tree mortality of species group i and diameter class j at time t, $m_{ijt} = P(M_{ijt} = 1|x)$, is estimated with a Probit function (Albert and Anderson, 1981). M_{ijtk} is a binary variable representing whether a tree of species i and diameter class j died ($M_{ijtk} = 1$) or not ($M_{ijtk} = 0$):

$$m_{ijt} = \Phi(\delta_{i1} + \delta_{i2}TCB + \delta_{i3}DI + \delta_{i4}EVI + \delta_{i5}SWIR + \delta_{i6}TCG + \delta_{i7}SAVI + \delta_{i8}TCA + \delta_{i9}E + \delta_{i10}S + \delta_{i11}cosA + \delta_{i12}sinA + \xi_{ij}) \quad (7)$$

where Φ is the standard normal cumulative function, δ_i's are parameters estimated by maximum likelihood. $\xi$is an error term.

Harvesting probability of species group i and diameter class j at time t, $h_{ijt} = P(H_{ijt} = 1|x)$, is also estimated with a Probit function. H_{ijtk} is a binary variable representing whether a tree of species i and diameter class j harvested ($H_{ijtk} = 1$) or not ($H_{ijtk} = 0$):

$$h_{ijt} = \varpi(\partial_{i1} + \partial_{i2}TCB + \partial_{i3}DI + \partial_{i4}EVI + \partial_{i5}SWIR + \partial_{i6}TCG + \partial_{i7}SAVI + \partial_{i8}TCA + \partial_{i9}E + \partial_{i10}S + \partial_{i11}cosA + \partial_{i12}sinA + \infty 0_{ij}) \quad (8)$$

where$\varpi$is the standard normal cumulative function, ∂_i's are parameters estimated by maximum likelihood. $\infty$is an error term.

Recruitment of species group i, R_i is estimated with a Tobit model (Tobin, 1958):

$$R_{it} = \Phi(\beta_i x_{it}\sigma_i^{-1})\beta_i x_{it} + \sigma_i\phi(\beta_i x_{it}\sigma_i^{-1}) \quad (9)$$

with

$$\beta_i x_{it} = \beta_{i1} + \beta_{i2}TCB + \beta_{i3}DI + \beta_{i4}EVI + \beta_{i5}SWIR + \beta_{i6}TCG + \beta_{i7}SAVI + \beta_{i8}TCA + \beta_{i9}E + \beta_{i10}S + \beta_{i11}cosA + \beta_{i12}sinA + \mu_{ij} \quad (10)$$

where Φ is the standard normal cumulative distribution function and φ is the standard normal probability density function.$\mu$is an error term.

The densities of forest C pools (including AGB C, standing dead C, downed dead C, litter C, and soil organic C) are estimated with the following model (Ma et al., 2018b):

$$\psi_{it} = \omega_{i1} + \omega_{i2}TCB + \omega_{i3}DI + \omega_{i4}EVI + \omega_{i5}SWIR + \omega_{i6}TCG + \omega_{i7}SAVI + \omega_{i8}TCA + \omega_{i9}E + \omega_{i10}S + \omega_{i11}cosA + \omega_{i12}sinA + \omega_i \quad (11)$$

in which ψ_i is a vector of forest C pools including AGB C, standing dead C, downed dead C, litter C, and soil organic C, ω_i's are parameters to be estimated with the GLS. ω is an error term and ψ_i is calculated with Eq. (11).

In order to backcast forest population dynamics and associated forest C dynamics using matrix models from 2018 to 1990, we applied consistent annual rates of mortality, harvesting, and recruitment as forward predictions, but minus the annual rate of tree growth to enable backward validations. In addition, stand density was set to zero if stand age was less than 28 years. Annual effects of land cover changes were added every year from 1990 to 2018.

2.7. Model calibration and validation

We adopted the same variables and functional form for the underlying diameter growth, mortality, and recruitment models as those established in previously published matrix models (Ma et al., 2018b) to ensure accuracy and avoid overfitting and/or multicollinearity issues. A variety of stand level and Landsat variables selected for two species groups (deciduous and coniferous) were used in the matrix growth models (Table 2). Physiographic variables, elevation (E), slope (S), and aspect (A), were used to control for site productivity (Lennon et al., 2002). Landsat variables, tasseled cap brightness (TCB), disturbance index (DI), enhanced vegetation index (EVI), shortwave infrared surface reflectance ($SWIR$), greenness indices (TCG), soil adjusted vegetation index ($SAVI$), tasseled cap angle (TCA) were used to replace total stand basal area (B) as key predictors, due to their significant effects on forest C dynamics (Ma et al., 2018b). Model validation followed Ma et al. (2018b) where matrix models were used to produce suitable estimation of forest AGB dynamics to actual AGB dynamics incorporating Landsat data with elevation (E), slope (S), and aspect (A). Therefore, we applied

the matrix models to estimate and map forest C dynamics from 1990 to 2018.

In order to more thoroughly evaluate our matrix model predictions of forest C stocks, average AGB C and soil organic C were projected using the Forest Carbon Succession v2.0 (ForCsv2) extension for the LANDIS-II model (Dymond et al., 2002) at the second inventory (i.e. remeasured during 2013–2018). This extension allows researchers to estimate C in five pools for each living age-species cohort, plus nine dead organic matter, and soil pools for each species (Dymond et al., 2016). Furthermore, the accumulation of AGB C through growth and regeneration follow the Biomass Succession (v2) extension and the methods outlined in Scheller and Mladenoff (2004). Based on definitions of forest C pools, we only compared average AGB C and soil organic C predicted by matrix models and ForCsv2 in this study.

2.8. Land cover changes and forest C transfers

We used three general land cover categories as an initial approach to characterize land changes: forestland, cropland, and grassland. In this study, we used definitions from the IPCC Good Practice Guidance to classify land cover and land cover changes. Forestland includes all land with woody vegetation consistent with thresholds used to define forestland in the national GHG inventory, sub-divided into managed and unmanaged, and also by ecosystem type as specified in the IPCC Guidelines. Cropland includes arable and tillage land, and agro-forestry systems where vegetation falls below the thresholds used for the forestland category, consistent with the selection of national definitions. Grassland includes rangelands and pasture land that is not considered as cropland. Grassland also includes systems with vegetation that fall below the threshold used in the forestland category and are not expected to exceed, without human intervention, the threshold used in the forestland category. Afforestation includes land cover changes from cropland and grassland to forestland. Deforestation includes land cover changes from forestland to cropland and grassland. To more accurately estimate C gains/losses from land cover changes in the northern US, we used empirical transfer information from Zheng et al. (2011) which provided detailed transfer rate and precisely estimated forest area and C changes in the conterminous US including the northern US region associated with land cover change, harvest, and fire. Therefore, only transfers of AGB C and soil organic C were considered for afforestation and deforestation in this study. Carbon gains including soil C through afforestation were estimated using C accumulation tables for afforestation (Smith et al., 2006). Carbon losses through deforestation were estimated using average forest AGB C density from the FIA data, assuming that 20% of the aboveground forest C remained after forest became non-forest (Zheng et al., 2011). Soil C losses were calculated using soil C stocks (Smith et al., 2006) and a conversion loss of 0.25 for the 28-year period during 1990–2018. Since our study only focused on C stored or sequestrated in the forest land, transfers of C from harvested forests to harvested wood products were not considered when associated with land cover changes and harvests.

2.9. Fuzzy sets representing uncertainty

Uncertain land cover changes and harvests could lead to high variability in predicted values of forest C pools including AGB C, standing dead C, downed dead C, litter C, and soil organic C. The averages of predicted forest C are important point estimates but to understand the associated risk, ranges or sets indicating prediction uncertainty are essential. Here we used fuzzy sets which involved defining membership functions that determined the level of uncertainty (Zadeh, 1965). A trapezoidal fuzzy set was used, mathematically expressed as f (x; a, b, c, d) = max (min (x – ab – a, 1, d – xd – c), 0). [a, b] and [c, d] are the uncertainty intervals with membership degrees ranging from 0 to 1. [b, c] represents the certainty interval for which the membership degree is 1. [a, d] is a measure of total range of uncertainty

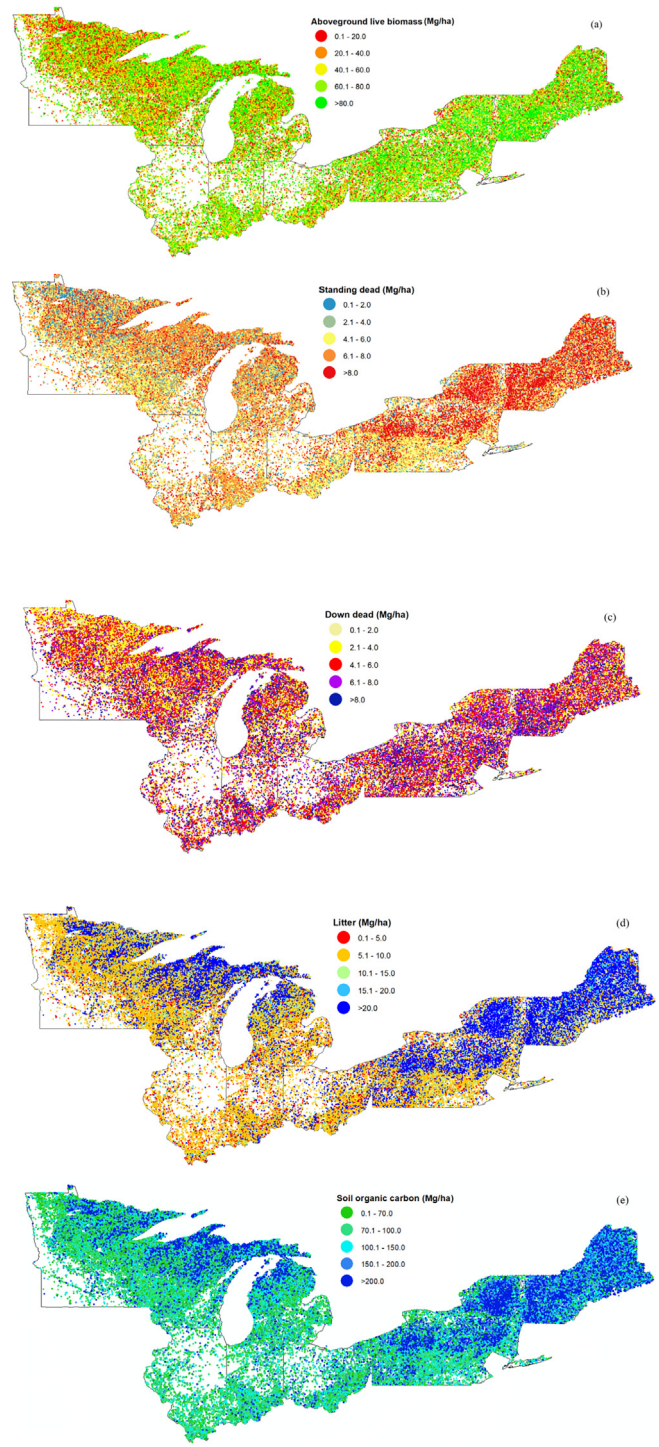

Fig. 1. Spatial distribution of AGB C density (a), standing dead C density (b), downed dead C density (c), litter C density (d), and organic soil C density (e) in forests across the northern US based on Forest Inventory and Analysis (FIA) plots during 2008–2018. (Note: 1 Mg ha^{-1} = 1 ton ha^{-1}).

arising from land cover change and harvest occurrences. Based on a prior study by Weckenmann and Schwan (2001), given the average value of predicted forest C ($\bar{X}$) and its relative standard deviation (S_r) from simulations, a, b, c, d values can be calculated as follows:

$$b = \frac{\bar{X}}{1 + 0.5S_r}$$
$$c = \bar{X}(1 + 0.5Sr)$$
$$a = b - \bar{X}\left(\frac{1}{1 + 0.5S_r} - \frac{1}{1 + 2.5S_r}\right)$$
$$d = c + \bar{X} \cdot 2Sr \quad (12)$$

3. Results

3.1. Average forest carbon density

The total forest C was composed of AGB C, standing dead C, downed dead C, litter C, and soil organic C pools in this study. Based on the FIA plots, average density of AGB C, standing dead C, downed dead C, litter C, and soil organic C were 62.29, 7.13, 6.52, 16.98, and 142.75, varied from the range of 0 to 896.32, 0 to 56.41, 0 to 72.67, 0 to 48.22, and 0 to 1123.56 ton ha^{-1}, respectively (Fig. 1). In addition, the forest C pools including AGB, standing dead, downed dead, litter, and soil were all positively skewed, with most estimates < 80, 20, 25, 15, 200 ton ha^{-1}, respectively. The spatial C density distributions of AGB, standing dead, downed dead, litter, and soil were displayed based on 78,458 plots across the northern US (Fig. 1). The northeast region and northern part of Minnesota, Wisconsin, and Michigan have higher C density than the rest of the study area.

3.2. Predictions of forest C pools

Based on the 15,692 validation plots, average AGB C, standing dead C, downed dead C, litter, and soil organic C predicted by the matrix models fell within the 95% confidence interval of the observed mean values at the second inventory, demonstrating high accuracy of the matrix models (Fig. 2). Compared to matrix models, the average AGB C and soil organic C predicted by the ForCsv2 both fell above the 95% confidence interval of the observed mean values, featuring an overestimate of C pools. Additionally, AGB C and soil organic C predicted by the matrix models and the ForCsv2, and standing dead C, downed dead C, and litter C predicted by the matrix models were compared with observed values (Fig. 3). Compared with the ForCsv2, the matrix models had 45% and 50% higher R^2, 43% and 38% lower MAPE for AGB C and soil organic C, respectively. Based on the substantially higher RMSE, MAPE and smaller R^2 than the matrix models, the ForCsv2 displayed much less accuracy of forest AGB and soil C predictions than the matrix models (Figs. 2 and 3).

3.3. Land cover changes

According to the NLCD, ~778 km^2 yr^{-1} of non-forest (grassland and cropland) converted to forestland whereas 1260 km^2 yr^{-1} of forestland changed to non-forest, resulting in a net loss of 482 km^2 yr^{-1} forestland across the northern US every year during 2001–2011 (Table 3). For each state, annual spatial variation in forest area change (afforestation + deforestation) due to the land cover change effects ranged from a 184 km^2 yr^{-1} forestland loss in Maine to a 45 km^2 yr^{-1} forestland gain in Minnesota across the northern US (Table 3). Additionally, Michigan had the highest afforestation area with 218 km^2 yr^{-1} and Vermont had the least deforestation area with 17 km^2 yr^{-1}.

3.4. Forest C changes under land cover changes and harvests

Land cover changes and forest harvests reduced forest C sink by 0.15 ton C ha^{-1} yr^{-1} and 0.38 ton C ha^{-1} yr^{-1}, accounting for 29% and 71% of C reductions across the study region (Table 4). Harvest activities accounted for higher annual C removals than land cover changes, an estimated difference of 0.22 ton C ha^{-1} yr^{-1}. However, forests remaining forests sequestered 2.38 Pg C with annual C sequestration of 1.94 ton C ha^{-1} yr^{-1} from 1990 to 2018, in which Pennsylvania had the greatest C sequestration with 0.35 ton C ha^{-1} yr^{-1} and Indiana had the least with 0.05 ton C ha^{-1} yr^{-1}. Considering land cover changes and harvests, forests of the northern US sequestered 1.73 Pg C (forest C changed from 6.23 to 7.96 Pg C) during 1990–2018, which is an annual rate of 0.88 ton C ha^{-1} yr^{-1} (Table 4 and Fig. 4). Net forest C gain had the highest value of 0.29 ton C ha^{-1} yr^{-1} in Pennsylvania and the lowest value of 0.03 ton C ha^{-1} yr^{-1} in Indiana (Table 4). In addition, the AGB C, standing dead C, downed dead C, litter C, and soil organic C comprised 15.99–23.10%, 3.17–3.45%, 2.30–2.54%, 2.47–2.83%, and 68.08–76.07% of total forest C across the northern US from 1990 to 2018.

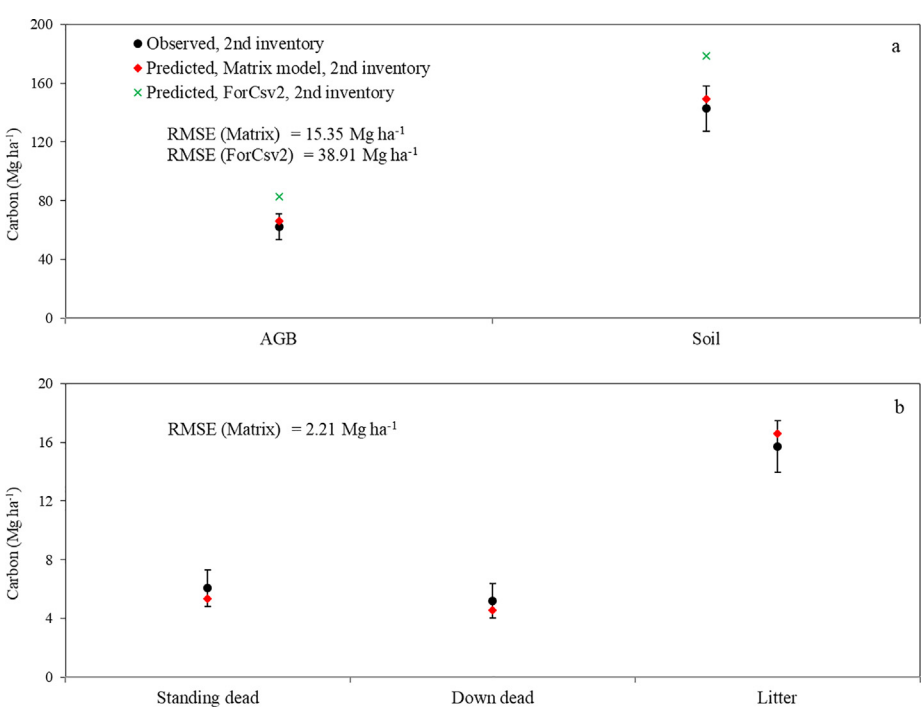

Fig. 2. Average predicted and observed AGB C and soil C at the second inventory of the matrix models and the ForCsv2 (a), average predicted and observed standing dead C, downed dead C, and litter C at the second inventory of the matrix models (b) with the 95% confidence interval of the observed mean values. Based on definitions of forest C pools, we only compared average AGB C and soil organic C predicted by matrix models and ForCsv2. (Note: 1 Mg ha^{-1} = 1 ton ha^{-1}).

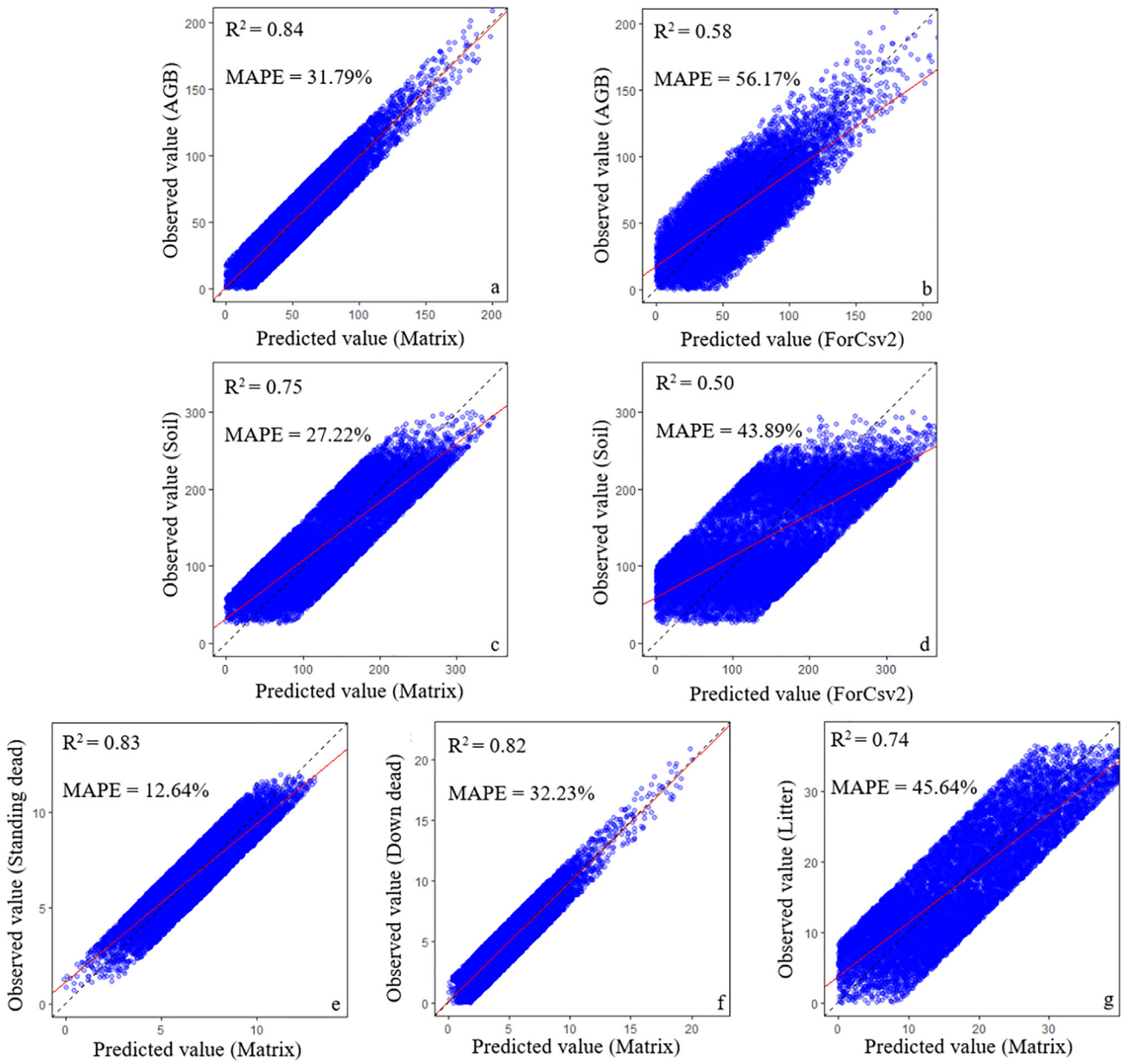

Fig. 3. Observed and predicted AGB C (a, b) and soil C (c, d) at the second inventory of the matrix models and the ForCsv2, observed and predicted standing dead C (e), downed dead C (f), and litter C (g) at the second inventory of the matrix models. Based on definitions of forest C pools, we only compared AGB C and soil organic C predicted by matrix models and ForCsv2.

3.5. Spatial characterizations of forest C

In consideration of land cover changes and harvests, the spatial distributions of C density of AGB, standing dead, downed dead, litter, and soil (ton ha^{-1}) across the northern US were characterized at a resolution of 200 m × 200 m based on improved matrix models (Fig. 5). The average density of AGB C, standing dead C, downed dead C, litter C, and soil organic C was 59.44, 6.06, 5.19, 15.73, and 138.27 ton ha^{-1}, respectively, during 1990–2018 (Fig. 5). The highest forest C stocks shown on the maps were predicted by the matrix models in three states: Maine, New Hampshire, and Vermont.

3.6. Uncertainty analysis

To quantify the uncertainty induced by land cover changes and harvests, fuzzy sets were constructed for repeating randomization processes to generate forest C uncertainty maps (Fig. 6). We examined the uncertainties of land cover change and harvest impacts on five forest C pools through model 12, which are represented by average value of predicted forest C and its relative standard deviation. Generally, the absolute uncertainties of land cover change and harvest impacts on standing dead C, downed dead C, and litter C were lower than 4.50 ton ha^{-1} (Fig. 6b, c, d). In comparison, high uncertainties of soil organic C and AGB C storage were at about 12–40 ton ha^{-1} in the northern Michigan, Wisconsin, Minnesota, and Maine, New Hampshire, and New York (Fig. 6a, e).

4. Discussion

4.1. Forest carbon estimation comparisons

The average density of AGB C, standing dead C, downed dead C, litter C, and soil organic C were 62.29, 7.13, 6.52, 16.98, and 142.75 ton ha^{-1}, respectively, in the northern US. Grouping the countries by

Table 3
Average annual land cover (km^2 yr^{-1}, percent of forest area change) in the northern US during 2001–2011 from the National Land Cover Database (NLCD). The land cover classification system is used by NLCD2011, which is modified from the Anderson Land Cover Classification System.

State	Aff[a]	Def[b]	Net[c]
Minnesota	162 (0.14%)	−117 (0.10%)	45 (0.04%)
Wisconsin	101 (0.13%)	−153 (0.20%)	−52 (0.07%)
Illinois	31 (0.04%)	−73 (0.09%)	−42 (0.05%)
Indiana	24 (0.05%)	−34 (0.07%)	−10 (0.02%)
Michigan	218 (0.27%)	−163 (0.20%)	55 (0.07%)
Ohio	53 (0.09%)	−121 (0.21%)	−68 (0.12%)
Pennsylvania	55 (0.09%)	−138 (0.21%)	−83 (0.12%)
New York	25 (0.04%)	−139 (0.20%)	−114 (0.16%)
Vermont	5 (0.04%)	−17 (0.13%)	−12 (0.09%)
New Hampshire	9 (0.07%)	−26 (0.20%)	−17 (0.13%)
Maine	95 (0.21%)	−279 (0.63%)	−184 (0.42%)
Total	778 (1.16%)	−1260 (2.24%)	−482 (1.08%)

Note: Aff = afforestation, Def = deforestation.
[a] Afforestation includes land area changes from cropland and grassland to forestland.
[b] Deforestation includes land area changes from forestland to cropland and grassland.
[c] Net change = Aff + Def.

Table 4
Annual forest C (1000 ton yr^{-1}) changes subject to land cover changes (LCC) and harvests in the northern US during 1990–2018.

State	Aff[a]	Def[b]	LCC[c]	Frf[d]	Harvest[e]	Net[f]
Minnesota	194	−838	−644	14,343	−3259	10,440
Wisconsin	123	−1258	−1135	14,506	−4153	9218
Illinois	35	−672	−637	4061	−921	2503
Indiana	28	−349	−321	3625	−1128	2176
Michigan	257	−1432	−1175	13,715	−3169	9371
Ohio	66	−1143	−1077	11,533	−1274	9182
Pennsylvania	69	−1379	−1310	23,910	−2632	19,968
New York	37	−1413	−1376	19,775	−2230	16,169
Vermont	9	−202	−193	4843	−101	4549
New Hampshire	13	−308	−295	5048	−1721	3032
Maine	157	−2318	−2161	16,767	−4928	9678
Total	988	−11312	−10324	132,126	−25516	96,286

Note: Aff = afforestation, Def = deforestation, Frf = forests remaining forests.
[a] Afforestation includes land area changes from cropland and grassland to forestland. C gains including soil C through afforestation were estimated using C accumulation tables for afforestation (Smith et al., 2006).
[b] Deforestation includes land cover changes from forestland to cropland and grassland. C losses through deforestation were estimated using average forest AGB C density from the Forest Inventory and Analysis (FIA) data, assuming that 20% of the aboveground forest C remained after forest became non-forest every year (Zheng et al., 2011). Soil C losses were calculated using soil C stocks (Smith et al., 2006) and a conversion loss of 0.25 for the 28-year period during 1990–2018.
[c] $LCC = C_{Aff} + C_{Def}$.
[d] C sequestration by forests remaining forests was estimated using matrix models.
[e] Effects of harvest (excluding the amount of C stored in wood products) on C sequestration using matrix models.
[f] Net C change = $C_{Aff} + C_{Def} + C_{Frf} + C_{Harvest}$. Negative numbers indicate carbon sources (i.e. sum of annual C decrease) while positive numbers represent carbon sinks (i.e. sum of annual C increment).

main forest region in Europe, the average range of forest C (including C stored in stem, branch, foliage, and root) for all countries and stands is 153.2 ton ha^{-1} for *P. abies* and 171.2 ton ha^{-1} for *F. sylvatica*. with 30 cm DBH (Neumann et al., 2016a). Our results for AGB C is lower than European forest C estimates. In addition, our model estimated net annual forest C sequestration rate at 1.94 ton C ha^{-1} yr^{-1} during 1990–2018, falling in the range of historically reported estimates from 0.97 to 2.32 ton C ha^{-1} yr^{-1} (Birdsey et al., 1993; Turner et al., 1995; Heath et al., 2011; Zheng et al., 2011; Woodall et al., 2015b). Globally, it has been reported that the current forest C stock is estimated to be 861 ± 66 Pg C, with 42% in live biomass (above- and below-ground), 8% in deadwood, 5% in litter, and 44% in soil (a depth of 1 m) (Pan et al., 2011). In comparison, our predictions of AGB C, deadwood C, litter C, and soil organic C (a depth of 1 m) were made up 16–23%, 5–6%, 2–3%, and 68–76% of total forest C across the northern US from 1990 to 2018, respectively. Obviously, our results for soil organic C stocks are higher than global estimates, but AGB C, deadwood C, and litter C are all lower. However, our results are consistent with Woodall et al.'s (2015b) findings in terms of total C stocks in the continuous US. This improved empirical-based matrix modeling provided contemporary forest C predictions considering effects of land cover changes and harvests on diameter growth, mortality, and recruitment coupling with big datasets such as Landsat or large scale NFI data, which is in principle more accurate and reasonable. Therefore, forest C simulations using process-based models or other empirical models while considering disturbances should be carefully calibrated and validated using inventory data to avoid overestimation or underestimation in forest C predictions.

4.2. Consideration of uncertainty

Taking into consideration uncertainty is especially critical when studying the forest C dynamics because forests are highly complex dynamic ecosystems constantly intervened by human activities such as land cover changes and harvests (Miehle et al., 2006; Ma et al., 2019). In general, there are three uncertainty sources in forest C simulations, namely, parameter uncertainty, scenario uncertainty, and model uncertainty (Lloyd and Ries, 2007). Here, we focused on quantifying the parameter uncertainty from the land cover change and harvest impacts by incorporating detailed land cover change histories derived from the NLCD data and specified harvesting information from the NFI data in terms of fuzzy set theory which describes uncertainty in terms of membership degree (Weckenmann and Schwan, 2001). In this study, we used a two-step approach to estimate parameter uncertainty in the forest C predictions. First, Monte Carlo simulations (Fichthorn and Weinberg, 1991) were used to produce random realizations of possible parameters thus generating the average and relative standard deviation of outputs. Then uncertainty in forest C predictions from land cover changes and harvest activities in terms of fuzzy sets determined the level of output uncertainty caused by uncertain parameter inputs. The uncertainty range of outcomes related to land cover changes and harvests indicated these human activities to be perhaps the most important uncertainty regarding the strength of the forest C sequestration.

Nevertheless, we only estimated the possible ranges in forest C predictions as an index of uncertainty from land cover changes and harvests due to the complexity of modeling human intervention processes in forests. In addition, we did not consider spatial auto-correlation for absolute uncertainties in this study. Admittedly, this study only considered very limited and narrow sources of uncertainty thus caution should be extended to applying the uncertainty as drivers of forest C flux. Therefore, more accurate and deeper sources of uncertainty can be explored to reduce uncertainty associated with forest C predictions. In all, it is a challenging task to account for numerous sources of uncertainty in forest C predictions based on matrix models.

4.3. Forest C storage changes and factors contributing to change

Forests comprise 65% of land area and are the largest terrestrial C sink on the planet (Pan et al., 2011). Deforestation and forest degradation, however, release a tremendous amount of the sequestrated C back to the atmosphere. The Intergovernmental Panel on Climate Change (IPCC) indicates that C emissions and removals associated with land use and cover changes can be attributed to specific activities (IPCC, 2013). In this study, we estimated that land cover changes

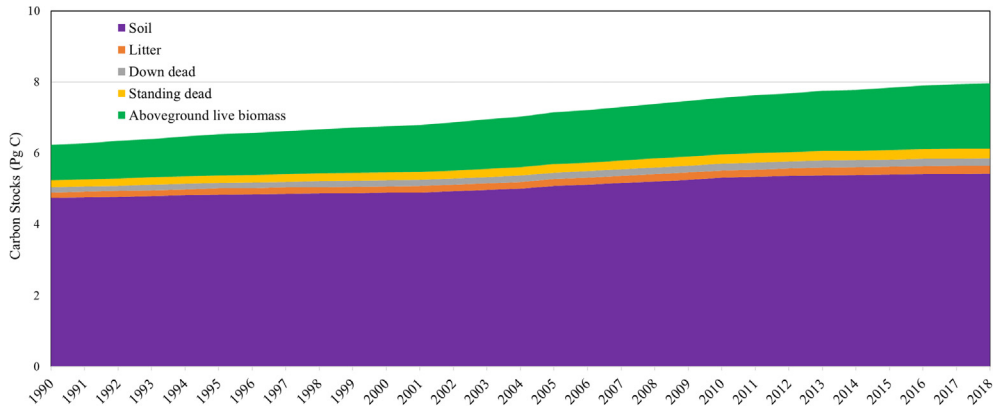

Fig. 4. Accumulated forest carbon storage changes in different pools subject to land cover changes and harvests from 1990 to 2018.

(afforestation + deforestation) reduced the forest C sink by 0.15 ton C ha^{-1} yr^{-1} during 1990–2018, accounting for 29% of C reductions across the northern US. Obviously, the periodic trend was a decline in forest C sink strength due to greater deforestation than afforestation without considering effects of forests remaining forests growth. Additionally, conversion between forestland and non-forestland resulted in a net loss of 482 km^2 yr^{-1} forestland across the northern US every year during 2001–2011. Such a large loss of forest area can be partly explained by the inaccurate distinction between deforestation and intensive management operations such as clearcutting regeneration techniques. As some deforestation might be inaccurately ascribed to forest management operations there would effectively be no change in land use (Woodall et al., 2016). Prior to 1985, uncertainty in land cover change data induced a wide margin of forest C estimates. Uncertainty in forest C estimates due to land cover change was reduced by nearly 50% after 1985, largely due to increased spectral and spatial resolution, improved mapping capabilities, and increased data availability (Sleeter et al., 2018). Additionally, our results should be interpreted in an appropriate context as we only focus on forest C changes in the forestland, but not C stored in the grassland and cropland. With the land cover changes, we only considered the major pools of AGB C and soil C transferred from grassland and cropland to forestland and from forestland to grassland and cropland. We did not consider the transfers of standing dead C, downed dead C, and litter C to and from different land cover categories. Therefore, our forest C simulations were subject to the bias caused by the changes in land cover. Although maintaining forestland via conservation easements will be one policy consideration in the future, additional approaches such as reforestation and afforestation might be needed to ensure terrestrial C accumulation within diverse land covers in a context of global change.

Forest harvesting transfers C within forest ecosystems from live to dead wood, and outside of forest ecosystems to atmosphere and harvest products (Sleeter et al., 2018). Although fluxes of C due to harvest activities varied over time, our study estimated that forest harvesting accounted for 71% of C reductions through harvest products across the study region, with a decline of forest C sink by 25.52 Tg C yr^{-1} (0.38 ton C ha^{-1} yr^{-1}) during 1990–2018. This C removal estimate of harvesting aligns with numerous other studies, largely based on FIA plots. For instance, the US Environmental Protection Agency (EPA) estimated harvest removals at 143 Tg C in 1990, 134 Tg C in 2000, and 95 Tg C in 2009 (EPA, 2011; Williams et al., 2012), whereas Sleeter et al. (2018) estimated the combined harvest + emission removal at 135, 133, and 84 Tg C yr^{-1} for the same years. More generally, forest harvest C removals have been estimated in a range of studies spanning different temporal periods and applying different modeling, and range from 90 to 150 Tg C yr^{-1} (Williams et al., 2016). Our C removal estimate of harvest is substantially lower than these studies as we only considered C transfers to harvested products, but did not consider transfers within forest ecosystems from live to dead wood and outside of forest ecosystems to atmosphere through direct C emissions across the entire nation. However, our results are consistent with a previous study (Zheng et al., 2011) which estimated forest harvest removals by 23.86–27.21 Tg C yr^{-1} during 1992–2001 covering the same states.

Prior studies have shown evidence of increases in biomass across many forest types caused by forest growth (Johnson et al., 2000; McMahon et al., 2010). In our study, we found that forests remaining forests growth would increase the forest C sink by 1.94 ton C ha^{-1} yr^{-1} during 1990–2018, that over offset the C reductions from land cover changes (0.15 ton C ha^{-1} yr^{-1}) and harvests (0.38 ton C ha^{-1} yr^{-1}) and therefore resulted in net C increments (1.41 ton C ha^{-1} yr^{-1}) in this area. This result indicated that the northern US region served as a C sink in the past 28 years when considering land cover changes and forest harvesting activities. Moreover, the estimated forest C transferred to harvested wood products was 0.33 ton C ha^{-1} yr^{-1}. The forest C transferred to the wood products pool can be considered an addition to the C stored in the forests. As a renewable resource, harvested wood products may be recycled and reclaimed for energy resulting in a slow decomposition process (Lippke et al., 2010). The cumulative C stored in these products is a substantial store of C as the wood products in buildings have lives of 80 yr or more (Winistorfer et al., 2007, US EPA, 2018).

4.4. Spatially explicit and continuous forest C estimation

Under the UNFCCC, the US is required to report GHG emissions and sinks each year from 1990 to near present (US EPA, 2018). Forest ecosystems alone account for over 80% of all terrestrial aboveground C and over 70% of the C stored in soil (Balshi et al., 2007). Due to the importance of forest C storage to the global C budget an understanding of the contemporary role of forest C sequestration in forests is required (Pan et al., 2011). Our study extended prior work (Woodall et al., 2015a,2015b; Domke et al., 2016, 2017; Ma et al., 2018a,2018b; Ma et al., 2019) from being limited to a plot-network to being spatially explicit and continuous across the northern US. Based on matrix models with NFI, Landsat, and DEM data, the average forest C density maps of AGB, standing dead, downed dead, litter, and soil during 1990–2018 contain much more spatial details than the plot-based forest C estimates (Woodall et al., 2015a,2015b; Domke et al., 2016, 2017; Ma et al., 2018a,2018b; Ma et al., 2019). Spatially explicit forest C estimates which are also spatially continuous are critical for future forest C modeling and forest C estimation. Additionally, our model predictions indicated that average forest C density in the New England region is 2–6 times larger than that of forest C pools in the Great Lakes region. This may be related to New England tree density being much higher than that of the Great Lakes region. This result is consistent with historical studies which suggested average forest C density of New England region

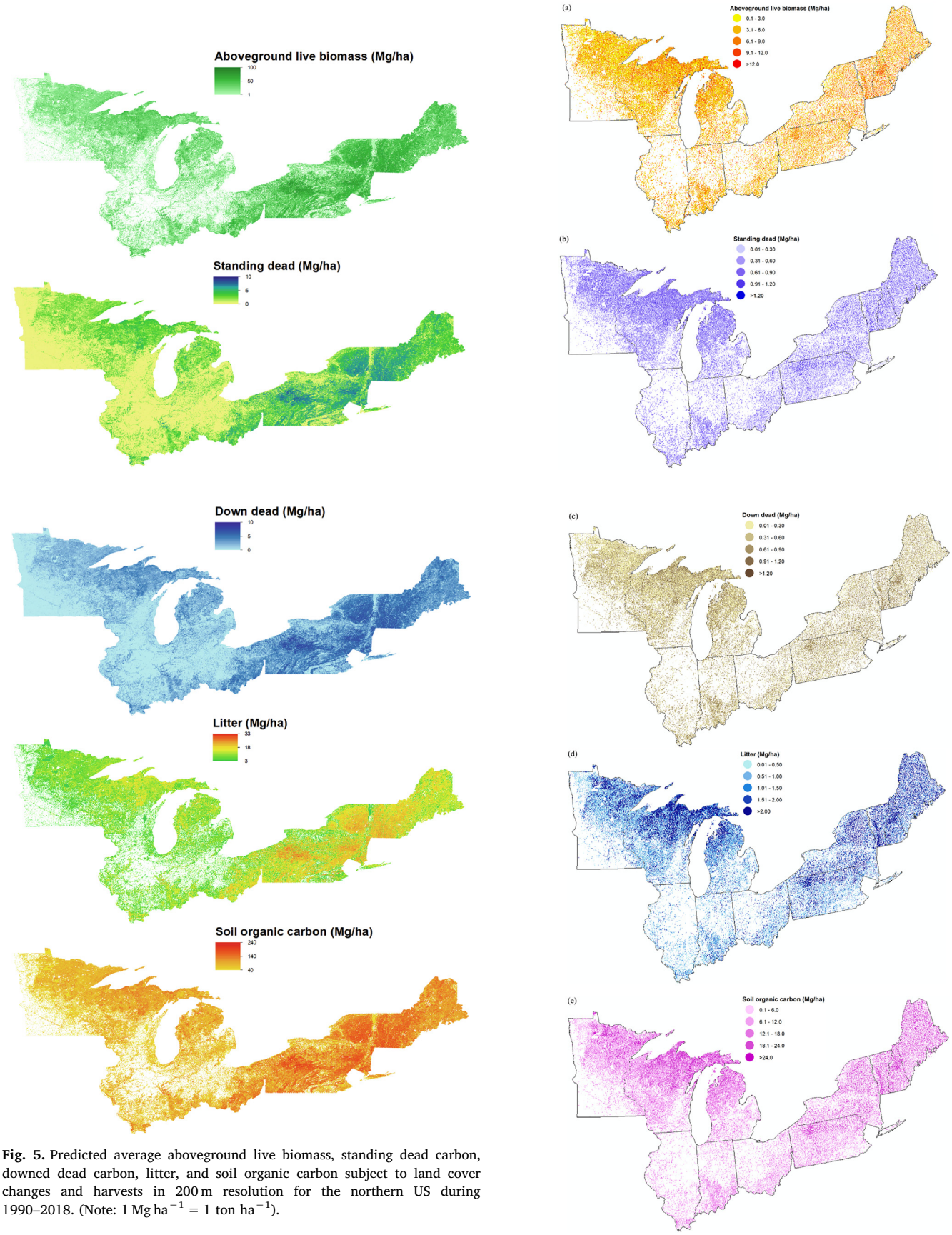

Fig. 5. Predicted average aboveground live biomass, standing dead carbon, downed dead carbon, litter, and soil organic carbon subject to land cover changes and harvests in 200 m resolution for the northern US during 1990–2018. (Note: 1 Mg ha^{-1} = 1 ton ha^{-1}).

(caption on next page)

Fig. 6. Absolute uncertainties (i.e. absolute values from uncertainty intervals of d – c or b – a in fuzzy set) in estimating impacts of land cover changes and harvests on aboveground live biomass, standing dead carbon, downed dead carbon, litter, and soil organic carbon for the northern US during 1990–2018. (Note: 1 Mg ha^{-1} = 1 ton ha^{-1}).

was greater than that of the Great Lakes region (Domke et al., 2017; Cao et al., 2019; Ma et al., 2019). Our study based on available NFI, Landsat, and DEM data using matrix models provided a baseline for future forest C estimates in the northern US. The data products developed in this study reflect C density estimates for all forest ecosystem pools for the period 1990 to 2018. These estimates can be used by state and local entities interested in forest C estimation and reporting. These products can also serve as a basis for comparison as new methods and models are developed to leverage high resolution, remotely sensed information with NFI data.

5. Conclusions

In this study we used matrix models coupled with NFI, Landsat, DEM, and NLCD data to estimate the spatial and temporal distributions of forest AGB C, standing dead C, downed dead C, litter C, and soil C in the northern US from 1990 to 2018 while considering land cover changes and harvests. We estimated land cover changes and forest harvesting reduced the forest C sink by 0.15 ton C ha^{-1} yr^{-1} and 0.38 ton C ha^{-1} yr^{-1}, accounting for 29% and 71% of forest C reductions over the study period. However, forests remaining forests sequestered 2.38 Pg C with annual C sequestration of 1.94 ton C ha^{-1} yr^{-1} from 1990 to 2018. Therefore, the net forest sink of the northern US increased 1.73 Pg C during 1990–2018, which is an annual rate of 0.88 ton C ha^{-1} yr^{-1}. In conclusion, our study provides foundations for future GHG estimation and reporting and opportunities to improve modeling, estimation, and attribution of forest C dynamics across spatial scales in support of inventory, monitoring, and reporting activities.

Declaration of Competing Interest

The authors declare that they have no known competing financial interests or personal relationships that could have appeared to influence the work reported in this paper.

Acknowledgements

This study was supported by the USDA Forest Service-Northern Research Station and the Department of Interior Northeast Climate Adaptation Science Center.

References

Albert, A., Anderson, J.A., 1981. Probit and logistic discriminant functions. Commun. Stat.-Theory Methods. 10, 641–657.
Alexander, P., Rabin, S., Anthoni, P., Henry, R., Pugh, T.A., Rounsevell, M.D., Arneth, A., 2018. Adaptation of global land use and management intensity to changes in climate and atmospheric carbon dioxide. Glob. Change Biol. 24 (7), 2791–2809.
Buongiorno, J., Michie, B.R., 1980. A matrix model of uneven-aged forest management. For. Sci. 26 (4), 609–625.
Birdsey, R.A., Plantinga, A.J., Heath, L.S., 1993. Past and prospective carbon storage in United States forests. For. Ecol. Manage. 58 (1–2), 33–40.
Balshi, M.S., McGuire, A.D., Zhuang, Q., Melillo, J., Kicklighter, D.W., Kasischke, E., Wirth, C., Flannigan, M., Harden, J., Clein, J.S., Burnside, T.J., McAllister, J., Kurz, W.A., Apps, M., Shvidenko, A., 2007. The role of historical fire disturbance in the carbon dynamics of the pan-boreal region: A process-based analysis. J. Geophys. Res. 112, G02029.
Cao, B., Domke, G.M., Russell, M.B., Walters, B.F., 2019. Spatial modeling of litter and soil carbon stocks on forest land in the conterminous United States. Sci. Total Environ. 654, 94–106.
Canham, C.D., Rogers, N., Buchholz, T., 2013. Regional variation in forest harvest regimes in the northeastern United States. Ecol. Appl. 23 (3), 515–522.
DeFries, R.S., Houghton, R.A., Hansen, M.C., Field, C.B., Skole, D., Townshend, J., 2002. Proc. Natl. Acad. Sci. 14256–14261.
Dymond, C.C., Scheller, R.M., Beukema, S., 2002. A new model for simulating climate change and carbon dynamics in forested landscapes, British Columbia. J. Ecosyst. Manage. 13, 1–2.
Dymond, C.C., Beukema, S., Nitschke, C.R., Coates, K.D., Scheller, R.M., 2016. Carbon sequestration in managed temperate coniferous forests under climate change. Biogeosciences 13, 1933–1947.
Domke, G.M., Woodall, C.W., Smith, J.E., 2011. Accounting for density reduction and structural loss in standing dead trees: Implications for forest biomass and carbon stock estimates in the United States. Carbon Balance Manage. 6 (1), 14.
Domke, G.M., Perry, C.H., Walters, B.F., Woodall, C.W., Russell, M.B., Smith, J.E., 2016. Estimating litter carbon stocks on forest land in the United States. Sci. Total Environ. 557, 469–478.
Domke, G.M., Perry, C.H., Walters, B.F., Nave, L.E., Woodall, C.W., Swanston, C.W., 2017. Toward inventory-based estimates of soil organic carbon in forests of the United States. Ecol. Appl. 27 (4), 1223–1235.
EPA, 2011. Inventory of US Greenhouse Gas Emissons and Sinks: 1990–2009. Washington, DC, USEP Agency.
Fichthorn, K.A., Weinberg, W.H., 1991. Theoretical foundations of dynamical Monte Carlo simulations. J. Chem. Phys. 95 (2), 1090–1096.
Goetz, S., Dubayah, R., 2011. Advances in remote sensing technology and implications for measuring and monitoring forest carbon stocks and change. Carbon Manage. 2 (3), 231–244.
Houghton, R.A., House, J.I., Pongratz, J., Van Der Werf, G.R., DeFries, R.S., Hansen, M.C., Quéré, C.L., Ramankutty, N., 2012. Carbon emissions from land use and land-cover change. Biogeosciences 9 (12), 5125–5142.
Houghton, R.A., 2003. Why are estimates of the terrestrial carbon balance so different? Glob. Change Biol. 9 (4), 500–509.
Harris, N.L., Hagen, S.C., Saatchi, S.S., Pearson, T.R.H., Woodall, C.W., Domke, G.M., Braswell, B.H., Walters, B.F., Brown, S., Salas, W., Fore, A., 2016. Attribution of net carbon change by disturbance type across forest lands of the conterminous United States. Carbon Balance Manage. 11 (1), 24.
Hasenauer, H., Nemani, R.R., Schadauer, K., Running, S.W., 1999. Forest growth response to changing climate between 1961 and 1990 in Austria. For. Ecol. Manage. 122 (3), 209–219.
Hasenauer, H., Petritsch, R., Zhao, M., Boisvenue, C., Running, S.W., 2012. Reconciling satellite with ground data to estimate forest productivity at national scales. For. Ecol. Manage. 276, 196–208.
Heath, L.S., Smith, J.E., Skog, K.E., Nowak, D.J., Woodall, C.W., 2011. Managed forest carbon estimates for the US greenhouse gas inventory, 1990–2008. J. Forest. 109 (3), 167–173.
Intergovernmental Panel on Climate Change (IPCC), 2013. Climate Change 2013: The Physical Science Basis. Working Group I Contribution to the IPCC 5th Assessment Report—Changes to the Underlying Scientific/Technical Assessment.
Jenkins, J.C., Chojnacky, D.C., Heath, L.S., Birdsey, R.A., 2003. National scale biomass estimators for United States tree species. For. Sci. 49, 12–35.
Johnson, C.M., Zarin, D.J., Johnson, A.H., 2000. Post-disturbance aboveground biomass accumulation in global secondary forests. Ecology 81 (5), 1395–1401.
Kurz, W.A., Dymond, C.C., White, T.M., Stinson, G., Shaw, C.H., Rampley, G.J., Metsaranta, J., 2009. CBM-CFS3: a model of carbon-dynamics in forestry and land-use change implementing IPCC standards. Ecol. Model. 220 (4), 480–504.
Le Quéré, C., Andrew, R.M., Canadell, J.G., Sitch, S., Korsbakken, J.I., Peters, G.P., Manning, A.C., Boden, T.A., Tans, P.P., Houghton, R.A., Keeling, R.F., 2016. Global carbon budget 2016. *Earth Syst. Sci. Data* (Online) 8 (2).
Law, B.E., Hudiburg, T.W., Berner, L.T., Kent, J.J., Buotte, P.C., Harmon, M.E., 2018. Land use strategies to mitigate climate change in carbon dense temperate forests. Proc. Natl. Acad. Sci 201720064.
Liang, J., Zhou, M., 2014. Large-scale geospatial mapping of forest carbon dynamics. J. Sustainable For. 33, 104–122.
Lloyd, S.M., Ries, R., 2007. Characterizing, propagating, and analyzing uncertainty in life-cycle assessment: a survey of quantitative approaches. J. Ind. Ecol. 11, 161–179.
Lennon, J.J., Kunin, W.E., Corne, S., Carver, S., Van Hees, W.W., 2002. Are Alaskan trees found in locally more favourable sites in marginal areas? Glob. Ecol. Biogeogr. 11, 103–114.
Lippke, B., Wilson, J., Meil, J., Taylor, A., 2010. Characterizing the importance of carbon stored in wood products. Wood Fiber Sci. 42, 5–14.
Ma, W., Liang, J., Cumming, J.R., Lee, E., Welsh, A.B., Watson, J.V., Zhou, M., 2016. Fundamental shifts of central hardwood forests under climate change. Ecol. Model. 332, 28–41.
Ma, W., Zhou, M., 2017. Assessments of harvesting regimes in central hardwood forests under climate and fire uncertainty. For. Sci. 64 (1), 57–73.
Ma, W., Woodall, C., Domke, G., D'Amato, A., Walters, B., 2018a. Stand age versus tree diameter as a driver of forest carbon inventory simulations in the northeast U.S. Can. J. For. Res. 480 (10), 1135–1147.
Ma, W., Domke, G., D'Amato, A., Woodall, C., Walters, B., Deo, R., 2018b. Using matrix models to estimate aboveground forest biomass dynamics in the Eastern USA through various combinations of LiDAR, Landsat, and forest inventory data. Environ. Res. Lett. 13 (12), 125004.
Ma, W., Domke, G., Woodall, C., D'Amato, A., 2019. Land use change, disturbance, and their interaction on forest aboveground biomass dynamics in the Northern U.S. Forests 10 (7), 606.
Miehle, P., Livesley, S.J., Li, C., Feikema, P.M., Adams, M.A., Arndt, S.K., 2006. Quantifying uncertainty from large-scale model predictions of forest carbon dynamics. Glob. Change Biol. 12, 1421–1434.
McMahon, S.M., Parker, G.G., Miller, D.R., 2010. Evidence for a recent increase in forest growth. Proc. Natl. Acad. Sci. 107 (8), 3611–3615.
Neumann, M., Zhao, M., Kindermann, G., Hasenauer, H., 2015. Comparing MODIS net

primary production estimates with terrestrial national forest inventory data in Austria. Remote Sens. 7 (4), 3878–3906.
Neumann, M., Moreno, A., Mues, V., Härkönen, S., Mura, M., Bouriaud, O., Merganič, J., 2016a. Comparison of carbon estimation methods for European forests. For. Ecol. Manage. 361, 397–420.
Neumann, M., Moreno, A., Thurnher, C., Mues, V., Härkönen, S., Mura, M., Bronisz, K., 2016b. Creating a regional MODIS satellite-driven net primary production dataset for European forests. Remote Sens. 8 (7), 554.
Ollinger, S.V., Aber, J.D., Reich, P.B., Freuder, R.J., 2002. Interactive effects of nitrogen deposition, tropospheric ozone, elevated CO2 and land use history on the carbon dynamics of northern hardwood forests. Glob. Change Biol. 8 (6), 545–562.
Pan, Y., Birdsey, R.A., Fang, J., Houghton, R., Kauppi, P.E., Kurz, W.A., Phillips, O.L., Shvidenko, A., Lewis, S.L., Canadell, J.G., Ciais, P., 2011. A large and persistent carbon sink in the world's forests. Science 333, 988–993.
Picard, N., Bar-Hen, A., Guédon, Y., 2003. Modelling diameter class distribution with a second-order matrix model. For. Ecol. Manage. 180 (1–3), 389–400.
Rao, C.R., 1973. Linear statistical inference and its applications. John Wiley, New York.
Sleeter, B.M., Liu, J., Daniel, C., Rayfield, B., Sherba, J., Hawbaker, T.J., Zhu, Z., Selmants, P.C., Loveland, T.R., 2018. Effects of contemporary land-use and land-cover change on the carbon balance of terrestrial ecosystems in the United States. Environ. Res. Lett. 13 (4), 045006.
Scheller, R.M., Mladenoff, D.J., 2004. A forest growth and biomass module for a landscape simulation model, LANDIS: design, validation, and application. Ecol. Model. 180 (1), 211–229.
Smith, J.E., Heath, L.S., Skog, K.E., Birdsey, R.A., 2006. Methods for calculating forest ecosystem and harvested carbon with standard estimates for forest types of the United States. Gen. Tech. Rep. NE-343. US Department of Agriculture, Forest Service, Northeastern Research Station, Newtown Square, PA, pp. 343 216.
Smith, J.E., Heath, L.S., 2008. Forest sections of the land use change and forestry chapter, and Annex. In: US Environmental Protection Agency, Inventory of US Greenhouse Gas Emissions and Sinks: 1990-2006. EPA 430-R-08-005. http://www.epa.gov/climatechange/ghgemissions/usinventoryreport/archive.htm (17 October).
Smith, J.E., Heath, L.S., 2002. A model of forest floor carbon mass for United States forest types. Res. Paper. NE-722. U.S. Department of Agriculture, Forest Service, Northeastern Research Station, Newtown Square, pp. 37.
Tobin, J., 1958. Estimation of relationships for limited dependent variables. Econ. Soc. 26, 24–36.
Turner, D.P., Koerper, G.J., Harmon, M.E., Lee, J.J., 1995. A carbon budget for forests of the conterminous United States. Ecol. Appl. 5 (2), 421–436.
US EPA, 2018. EPA year in review 2017-2018 report.
Woodall, C.W., Walters, B.F., Coulston, J.W., D'Amato, A.W., Domke, G.M., Russell, M.B., Sowers, P.A., 2015. Monitoring network confirms land use change is a substantial component of the forest carbon sink in the eastern United States. Sci. Rep. 5.
Woodall, C.W., Coulston, J.W., Domke, G.M., Walters, B.F., Wear, D.N., Smith, J.E., Andersen, H.E., Clough, B.J., Cohen, W.B., Griffith, D.M., Hagen, S.C., Hanou, I.S., Nichols, M.C., Perry, C.H., Russell, M.B., Westfall, J., Wilson, B.T., 2015b. The US forest carbon accounting framework stocks and stock change 1990-2016 Gen. Tech. Rep. NRS-154. U.S. Department of Agriculture, Forest Service, Northern Research Station, Newtown Square, PA, pp. 49.
Woodall, C.W., Heath, L.S., Domke, G., Nichols, M., 2011. Methods and equations for estimating volume, biomass, and carbon for trees in the US forest inventory, 2010. USDA Forest Service General Technical Report NRS-88.
Woodall, C.W., Walters, B.F., Russell, M.B., Coulston, J.W., Domke, G.M., D'Amato, A.W., Sowers, P.A., 2016. A tale of two forest carbon assessments in the eastern United States: Forest use versus cover as a metric of change. Ecosystems 19 (8), 1401–1417.
Weckenmann, A., Schwan, A., 2001. Environmental life cycle assessment with support of fuzzy-sets. Int. J. Life Cycle Assess. 6, 13–18.
Williams, C.A., Gu, H., MacLean, R., Masek, J.G., Collatz, G.J., 2016. Disturbance and the carbon balance of US forests: A quantitative review of impacts from harvests, fires, insects, and droughts. Global Planet. Change 143, 66–80.
Williams, C.A., Collatz, G.J., Masek, J., Goward, S.N., 2012. Carbon consequences of forest disturbance and recovery across the conterminous United States. Global Biogeochem. Cycles 26 (1).
Winistorfer, P., Chen, Z., Lippke, B., Stevens, N., 2007. Energy consumption and greenhouse gas emissions related to the use, maintenance, and disposal of a residential structure. Wood Fiber Sci. 37, 128–139.
Yan, X., Zhao, J., 2007. Establishing and validating individual-based carbon budget model FORCCHN of forest ecosystems in China. Acta Ecol. Sinica 27 (7), 2684–2694.
Yu, Z., Lu, C., Cao, P., Tian, H., 2018. Long-term terrestrial carbon dynamics in the Midwestern United States during 1850–2015: Roles of land use and cover change and agricultural management. Glob. Change Biol. 24 (6), 2673–2690.
Zheng, D., Heath, L.S., Ducey, M.J., Smith, J.E., 2011. Carbon changes in conterminous US forests associated with growth and major disturbances: 1992–2001. Environ. Res. Lett. 6 (1), 014012.
Zheng, D., Heath, L.S., Ducey, M.J., 2008. Satellite detection of land-use change and effects on regional forest aboveground biomass estimates. Environ. Monit. Assess. 144 (1–3), 67–79.
Zheng, D., Heath, L.S., Ducey, M.J., Smith, J.E., 2013. Forest carbon dynamics associated with growth and disturbances in Oklahoma and Texas, 1992–2006. South. J. Appl. For. 37 (4), 216–225.
Zhang, F., Chen, J.M., Pan, Y., Birdsey, R.A., Shen, S., Ju, W., He, L., 2012. Attributing carbon changes in conterminous US forests to disturbance and non-disturbance factors from 1901 to 2010. J. Geophys. Res. Biogeosci. 117 (G2).
Zadeh, L.A., 1965. Fuzzy sets. Inf. Control 8, 338–353.